Powders and Grains (2005) – García-Rojo, Herrmann and McNamara (eds)
© 2005 Taylor & Francis Group, London, ISBN 0 415 38348 X

Compaction bands as observed in DEM simulations

G. Marketos & M.D. Bolton
Centre of Geotechnical Process and Construction Modelling, Cambridge University Engineering Department, UK

ABSTRACT: The recovery of oil from certain deep sub-sea reservoirs can be compromised by the formation of compaction bands in the reservoir sandstone. These bands may be relatively thin but of wide extent, and are thought to form in planes normal to the major principal stress. The native sand grains are found to have been severely crushed within such bands, producing a blanket of much reduced permeability. The underlying physics is not well understood. Discrete Element Modelling (DEM) has been used to study the initiation and propagation of compaction bands. Initial trials have been completed using the simplifying notion that a crushed grain immediately reduces to fragments an order of magnitude smaller than the parent grain. Compaction bands were seen to be associated with drops in the observed stress-strain curve coinciding with a swarm of crushing events. They formed against the smooth "platens", where the coordination number of grains is smaller. Similar observations have previously been made in physical tests.

1 INTRODUCTION

1.1 *Field evidence*

Compaction bands are thin zones of localised deformation that have very recently (Mollema & Antonellini, 1996) been identified in high-porosity sandstones. They are different to shear bands in that they accommodate pure compaction and hence porosity reduction with no shear of the top relative to the bottom layer. Their thickness is of the order of a few centimetres while they have been found to extend laterally over tens of meters in the field. They have been observed to occur in arrays of almost parallel bands with a spacing ranging from 4 to 50 centimetres. Inside these specific compaction bands Mollema & Antonellini (1996) observed microfracturing and some crushing of individual grains, while the porosity reduced from 20–25% to just a few %.

1.2 *Experimental investigation*

A large number of triaxial stressing experiments on samples of high-porosity sandstones have reproduced compaction bands in the laboratory (e.g. Baud et al. 2004; DiGiovanni et al. 2001; Olsson et al. 2002). Such experiments generated significant drops in the stress-strain curves. Acoustic emission monitoring associated these instabilities with an increase in the numbers of grains cracking and crushing.

Di Giovanni et al. (2001) found that the microstructure inside the sample displayed thin discrete zones of severe grain crushing (compaction bands), while the bulk of the material showed little deformation. On the other hand, Ollson et al. (2002) report localised compaction to be more diffuse, corresponding to an ever-increasing zone possibly made up of a number of inter-connected discrete bands, moving inwards.

In all cases compaction bands were found to form approximately in a direction perpendicular to the principal stress. In almost all cases they formed close to the top or bottom boundaries of the specimen. This is because the different contact force conditions, with lower coordination numbers and a less dense soil fabric, favour initiation of localisation in these zones. Vaidova & Wong (2003), however, reproduced internal compaction bands by inserting a circumferential notch (as a defect) in their sandstone specimens.

It should be noted that, depending on the mineralogical composition of the rock, localised compaction can be also generated by large grain rotations and rearrangement with almost no inter-granular breakages. However, here we will only be considering the case where grain crushing is the dominant micromechanism responsible for pore space collapse.

1.3 *Continuum mechanics approach*

Analysis of the conditions for compaction band initiation from a continuum mechanics point of view have associated this kind of localisation with a particular flow-rule for compaction at the yield envelope of a material (e.g. Olsson et al. 2002). This gives a new form of localisation, and it is possible that it can occur in unbounded granular matter such as sand. As such, compaction bands might provide a deformation mechanism for a variety of macroscopic processes. Most continuum mechanics approaches have used the strain localisation theory of Rudnicki & Rice (1975) to predict the direction of initial propagation of a band. They confirmed that a compaction band will form on a plane almost perpendicular to the principal stress direction.

1.4 *Micromechanics approach*

However continuum mechanics methods could not predict how localisation would develop (propagate) inside a band. An answer to this question will be sought by making use of a discrete approach, based on a better understanding of the perturbations upon the stress-carrying (strong-force) network caused by individual crushing events. A key element of such an approach is the reproduction of a compaction band in a discrete element simulation, as will be described here.

A set of similar such 'numerical experiments' will shed light on the micromechanical parameters that influence the formation of a compaction band (porosity, crushing strength, variability of grains). In addition it will give insight to the way a compaction band propagates. Finally the development of a mathematical model predicting which rock types and what conditions will give rise to a certain magnitude of instability might become possible.

2 THE DISCRETE ELEMENT METHOD

The discrete element code PFC^{3D} developed by Itasca Inc. was used for the simulations described here. A concise description of this code can be found in the PFC^{3D} manual (Itasca Inc, 2003). The sample used here is cuboidal (porosity 44.8%, initial dimensions 6 cm × 6 cm × 7.2 cm). It consists of 8943 spherical particles of radii uniformly distributed between 1 and 2 mm. It was prepared by a simulated 'numerical dry pluviation' and is bounded by frictionless walls on all sides. It should be noted that no gravity forces were included in this model and a soft contact approach was used. The side walls were kept stationary while a constant axial shortening rate of 0.1 m/s was applied. The micromechanical parameters used in these simulations can be found in Table 1. It should be noted that these values are of the order of magnitude inferred from single crushing tests on quartz particles reported by Nakata et al. (1999).

Crushing events were simulated as follows. A characteristic crushing stress parameter was assigned to each particle (here uniform, set as 40 MPa). The characteristic stress inside a particle, defined as the maximum normal contact force divided by the square of the diameter (following Nakata et al. 1999) was monitored throughout the simulation. A particle was then completely removed, so as to simulate crushing,

Table 1. Micromechanical parameters used for the simulation.

Parameter	Numerical Value
normal and shear stiffness of balls	4×10^6 N/m
normal and shear stiffness of walls	4×10^6 N/m
particle friction coefficient, μ_b	0.5
wall friction coefficient, μ_w	0.0
density of spheres	2650 kg/m^3
coefficient of local damping	0.7
sample shortening rate	0.1 m/s
particle 'crushing strength'	40 MPa

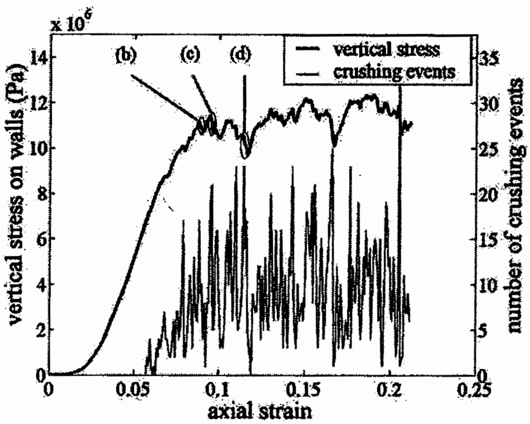

Figure 1. The vertical stress and number of crushing events (similar to acoustic emission data) plotted versus strain.

when its characteristic stress exceeded its characteristic strength. This represents small fragments, produced by crushing, falling into the pore space and losing their force-carrying capacity.

3 RESULTS

These simulations yielded the stress-strain curve of Figure 1. A history of crushing events similar to acoustic emission data reported in experiments (e.g. Baud et al. 2004) is also included. The initial response up to 0.02 strain is mostly due to particle rearrangement and to a lesser extent to elastic shortening at the contacts. Crushing of particles is initiated at a strain of 0.05. It reaches a constant mean level of about 10 events per 0.0008 strain interval, as shortening is dominated by particle crushing after a strain of roughly 0.09.

The stress-strain curve exhibits instabilities. Its peaks and drops can be associated with peaks and drops in the number of crushing events observed. Figure 2 plots the locations of the crushing events corresponding with these drops (i.e. points marked (b), (c) and (d) on Figure 1) indicating that at each

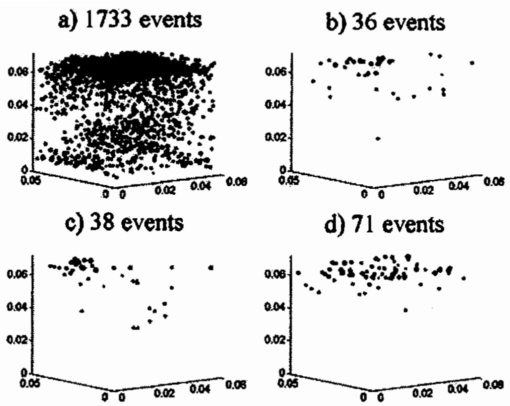

Figure 2. A plot of the location of crushing events inside the cubical element for a strain increment of (a) the whole run and (b), (c), (d) as marked on Figure 1.

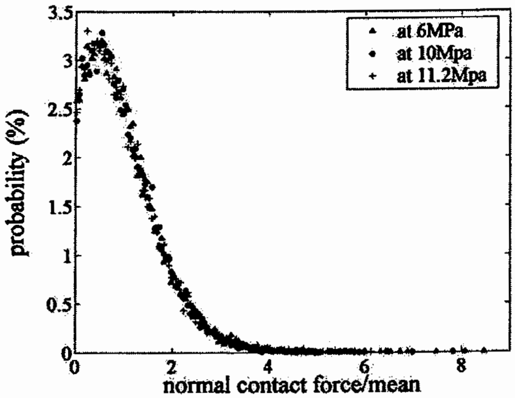

Figure 3. A plot of the probability density function of the normal contact force (as non-dimensionalised by the mean force) for three different stress and hence crushing levels.

specific instant particle and hence pore collapse is fairly localised within a band.

A plot of all the particle crushing events is included in Figure 2a. One can see here that crushing is not localised as a whole, although more crushing is observed towards the top of the specimen, corresponding to the location of compaction band formation. Crushing events occurring outside this region were found to correspond to instants of strain-hardening after a stress drop.

Considering an individual compaction band one can observe that it is associated with a surge in the number of crushing events and a stress drop, as observed in experiments. Particle crushing causes a severe disruption to the stress-carrying network of the sample, by removing the highest-stressed link in the strong-force network. The force carried by the crushed particle will redistribute itself to neighbouring particles (neighbouring links in the stress network). Depending on the packing and on the stress level, this might cause a crushing avalanche, by locally removing links lying roughly on the same plane normal to the major principal compressive stress. This would severely damage the stress-carrying ability of the sample, thus producing a stress drop in the strain-controlled test, as observed.

As crushing will remove the highest stressed particles it might be beneficial to consider the force distribution inside the specimen. The large-force part of this probability distribution was found to be approximated by an exponential function, as reported in various studies (Thornton, 1997; Radjai, et al. 1996), although the picture is not so clear for large-force events. A plot of the force distribution for the case of zero crushing (at a stress of 6 MPa), moderate (at 10 MPa, 85 crushed particles) and significant crushing (at 11.2 MPa, 1733 crushed particles) is shown on Figure 3.

It should be noted that the plots on Figure 3 are almost identical, apart from being chopped at large forces. As crushing becomes possible in the sample, the probability density function for normal contact force, which was initially essentially unbounded, now has to be limited by some value. This value depends on the stress level and the crushing strength of the particles. As the mean particle force increases, its limiting value when non-dimensionalised will become smaller.

4 DISCUSSION

Initial analyses of simulations which showed a significant degree of crushing would be in terms of bounded probability distributions like the one of Figure 3. An investigation into the problem of compaction bands would however need a more detailed analysis. Crushing would locally perturb the force distribution inside the sample and the condition for crushing localisation would depend on how large and how local this perturbation is.

A thorough investigation of these processes would require a good description of the spatial characteristics of the force distribution and perturbations to it. Such perturbations would have to be investigated as a function of micromechanical parameters such as the density of the fabric (or porosity), coordination number, the presence of cementation, etc.

An understanding of compaction band formation would be advantageous for the oil industry, as compaction bands have been encountered in sandstone. The reduction of porosity inside a compaction band is severe; as a consequence the overall fluid flow is highly choked. Knowledge of the parameters affecting compaction localisation and its propagation might help improve the efficiency of oil abstraction, or at least predict when problems might arise.

More specifically, the oil extraction process involves pore-pressure reduction, causing an effective stress increase in the parent rock. Careful drilling might therefore be able to control the 3D effective stress state and hence control the direction of formation of compaction bands so that flow is forced towards the well. In addition, compaction banding might shed light into the general area of reservoir compaction, as discussed by Nagel (2001).

It seems that under some circumstances compaction bands can also occur in unbounded granular material. Cheng (2004) observed the successive fragmentation of silica sand grains against a glass platen in one-dimensional compression. Fragments were so small that they could fall into the large voids below, between uncrushed parent grains. More work is needed so as to relate experimental observations to numerical simulations.

It should also be noted from the positioning of localisation as seen on Figure 2 that our initial simulations have produced compaction bands on or very close to the external boundary of the sample. This is due to the different stress conditions and different packing of the particles as induced by the flat platen. This was also observed in the laboratory tests with compaction bands concentrating towards the ends of the specimen. Future work will try to eliminate this artefact, by altering the boundary conditions. Initial simulations performed with this goal on the same sample have shown that there were no compaction bands forming if the boundary walls were significantly less stiff than the particles.

It should finally be noted that there is a limitation to the extent to which particle removal can simulate crushing. For small strains this is fine, as the fragments will fall into the void space and will not participate in the load carrying network if their volume is smaller than the void. They will merely block the pores reducing porosity. The accumulated fragments will, however, carry force after a high level of strain, and this stiffening effect has been neglected here. The position of previous crushing events and compaction bands will then affect the position of subsequent localisations. They would not, as here, be observed to form always at the same point. It is thought however that this should not affect the characteristics of the individual localisation events, as each one occurs throughout a very small strain increment, on a sample that is essentially uncrushed. Future work will be devoted to other ways of simulating crushing.

5 CONCLUSIONS

The simulations reported here have reproduced compaction bands caused by crushing of particles. Monitoring of the micromechanical parameters has associated the drops in the stress-strain curve with an increase in the number of crushing events, confirming experimental data. This is thought to be happening as a single crushing event causes an avalanche of local crushing as the stress carrying network redistributes itself. This depleted layer of particles is perpendicular to the macroscopic principal stress. Research is still needed to refine this numerical model, while an investigation of the parameters governing compaction band formation needs yet to be completed.

ACKNOWLEDGMENTS

The authors would like to thank the A.S. Onassis Foundation and the A.G. Leventis Foundation for their generous financial support.

REFERENCES

Baud P., Klein E. & Wong T.-F. (2004): Compaction localization in porous sandstones: spatial evolution of damage and acoustic emission activity, *Journal of Structural Geology*, 26,(3): 603–624.

Cheng Y. P. (2004): Micromechanical investigation of soil plasticity. PhD Thesis, Cambridge University, U.K.

DiGiovanni A. A., Fredrich J. T., Holcomb D. J. & Olsson W. A. (2001): Microscale damage evolution in compacting sandstone. *Fracture, Damage and Related Deformation Features*, Geological Society of London Special Publication, G. Couples, P. Meredith, and I. Main (Eds)

Itasca Consulting Group, Inc. (2003): *PFC^{3D}: Particle Flow Code in 3 Dimensions, Version 3.0*, Minneapolis, U.S.A.

Mollema P. N. & Antonellini M. A. (1996): Compaction bands: a structural analog for anti-mode I cracks in Aeolian sandstone. *Tectonophysics*, 267: 209–228.

Ollson W. A., Holcomb D. J. & Rudnicki J. W. (2002): Compaction Localization in Porous Sandstone: Implications for Reservoir Mechanics. *Oil and Gas Science Technology, Revue de l'Institut Français du Petrole*, 57: 591–599.

Nagel N. B. (2001): Compaction and subsidence issues within the petroleum industry: from Wilmington to Ekofisk and beyond, *Physics and Chemistry of the Earth (A)*, 26 (1–2): 3–14.

Nakata Y., Hyde A. F. L., Hyodo M., Murata H. (1999): A probabilistic approach to sand particle crushing in the triaxial test, *Geotechnique*, 49 (5): 567–583.

Radjai F., Jean M., Moreau J.-J. & Roux S. (1996): Force distributions in dense two-dimensional granular systems, *Physical Review Letters*, 77 (2): 274–277.

Rudnicki J. W. & Rice, J. R. (1975): Conditions for the localization of deformation in pressue-sensitive dilatant materials. *Journal of the Mechanics and Physics of Solids*, 23: 371–394.

Thornton C. (1997): Force transmission in granular media, *KONA*, 15: 81–90.

Vajdova V. & Wong T.-F. (2003): Incremental propagation of discrete compaction bands: Acoustic emission and microstructural observations on circumferentially notched samples of Bentheim, *Geophysics Research Letters*, 30 (14): 1775–1778.